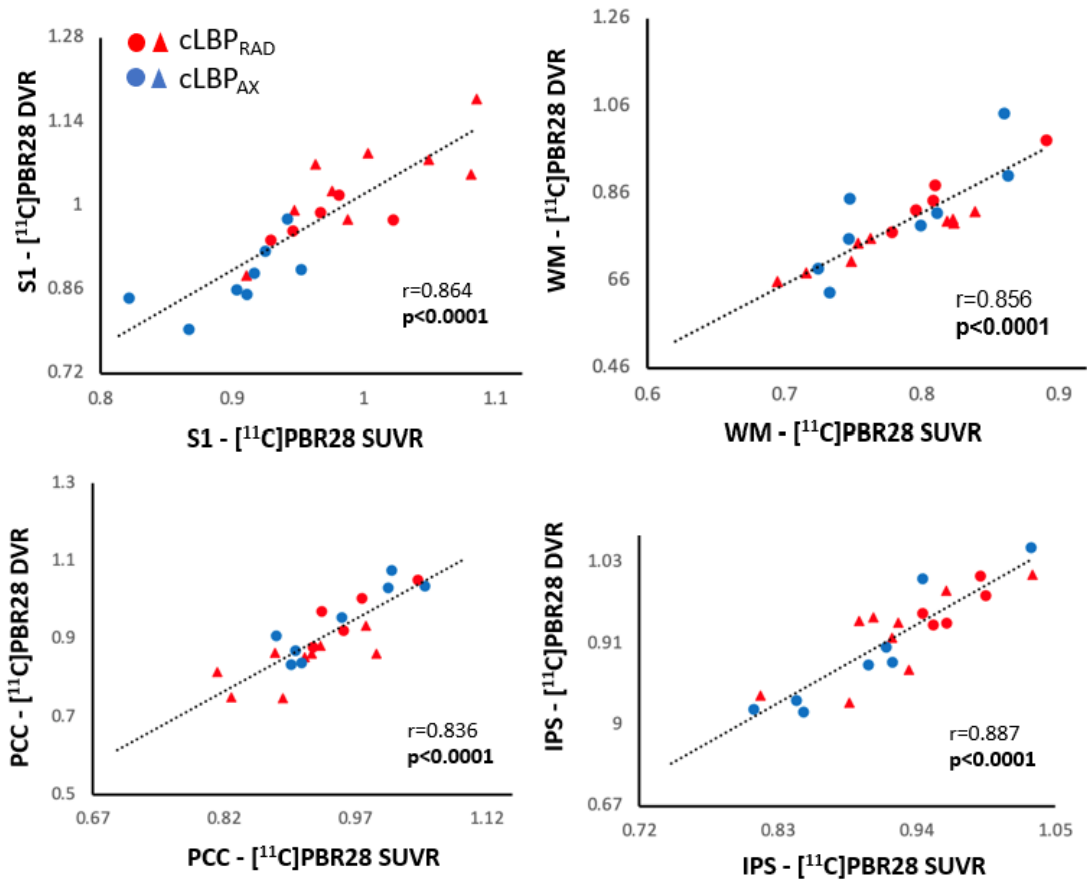


Methods

Blood metabolite analysis: For samples collected at 5, 10, 20, 30, 50, 70, and 90 minutes post- $[^{11}\text{C}]\text{PBR28}$ injection, blood was immediately separated under centrifugation (4,000 g; 4 min; 4°C) for each time point. In 18 patients, arterial blood processing was performed as previously described using a HyperSep C18 solid extraction cartridge to separation of radiometabolites.⁴⁵ In 4 patients, arterial blood was processed as follows. After centrifugation, 1 mL of plasma was added to 1 mL of acetonitrile and vortexed 3 times for 3 secs each. Protein precipitate was separated by centrifugation (4,000 g; 4 min; 4°C) then 1 mL of organic supernatant was added to 4 mL of water, vortexed, and injected (5 mL) onto High Performance Liquid Chromatography (HPLC) for separation of radiometabolites from parent radiotracer. The HPLC was configured with a column-switching valve for sample concentration (online solid phase extraction SPE; Agilent Bond Elut Online SPE, PLRP-S, 4.6 x 12.5 mm) followed by separation (Agilent Eclipse Plus C18, 4.6 x 100 mm. 3.5 μm). Configuration of the radiometabolite HPLC was modeled from previously reported methods.⁹¹ Briefly, each plasma sample was injected and trapped onto the SPE concentrator column with 1% ACN / 99% H₂O at 2mL/min for 3min. After 3 min, the sample was reverse eluted from the SPE column onto the separation column under gradient conditions (Mobile Phase A: water + 0.1% formic acid; Mobile Phase B: acetonitrile + 0.1% formic acid; separation method = 95/5 - 50/50 A/B from 3 – 8 min linear gradient; 50/50 – 5/95 A/B from 8-10 min linear gradient; 5/95 A/B from 10-11min isocratic; flow rate 2 mL/min). Radioactive analytes were monitored from 0-11 min after sample injection by dual opposing bismuth germanium oxide detectors for coincidence detection (Eckert and Ziegler). RadioHPLC chromatograms for each plasma sample analysis were decay-corrected and integrated to measure area under the curve for each radioactive metabolite compared to the parent radiotracer.

The parent fraction from each plasma sample from both analysis methods was fitted and applied to the plasma input curve resulting in a radiometabolite-corrected plasma input function. As two methods were used for blood processing in the analysis, blood was processed using both methods, and V_T was extracted from all target regions in 4 patients (1 included in this study, and 3 from different studies) to validate the use of both methods. V_T from the first blood processing method was significantly correlated against from the second blood processing method V_T ($0.995 \leq r \leq 0.999$; $p \leq 0.005$), allowing us to combine our data to increase statistical power in our study.

Electrical Stimulation: Each patient underwent two separate stimulation runs, each lasting 5 minutes 38 seconds. In each run, participants received 5 electric current stimuli, for each of the three body regions, i.e. back, right leg and left leg (pseudo-randomized order). For the back stimulation, electrodes were placed on the left and right of the fourth lumbar spine vertebra; for the right and left leg, electrodes were positioned on the lateral and medial sections of the knee. Each electrical stimulus was applied for 2 seconds at 35 Hz, at either 5mA (first run) or 12mA (second run). Stimuli were delivered using a TENS unit (Empi 300pv electrotherapy system) controlled with an in-house script using LabVIEW 16, Austin, Texas. Each stimulus was delivered 4-8s (jittered) after a visual anticipatory cue, indicating the body part about to be stimulated (indicated by the words “Back” “Right leg”, or “Left leg” projected in black onto a white background). Visual stimuli were presented using E-Prime (version 2.0). At the completion of each run, patients were asked to rate the average pain intensity (0 indicating no pain and 100 indicating worst pain tolerable) at each site. Please note that in the present study, we will only present the results of the 12mA (the strongest stimulation condition, thus more reliable to serve as a somatosensory functional localizer), whereas the 5mA run and the anticipatory cues are beyond the scope of the current investigation.



Supplementary Figure 1: [¹¹C]PBR28 signal (SUVR) correlations with distribution volume ratio (DVR). Data extracted from regions identified as statistically significant in voxel-wise group differences in [¹¹C]PBR28 SUVR. S1: primary somatosensory cortex; WM: white matter; PCC: posterior cingulate cortex; IPS: intraparietal sulcus. Triangle denotes data from protocol 1, circle denotes data from protocol 2. Red and blue denote cLBP_{RAD} and cLBP_{AX} patients, respectively.

Supplementary table 1 Regions of interest imaging values from two protocols.

		Protocol 1		Protocol 2	
		Radicular	Axial	Radicular	Axial
[¹¹ C]PBR28 SUVR PET signal	S1	0.98 ± 0.06*	0.91 ± 0.05	0.96 ± 0.05**	0.90 ± 0.05
	IPS	0.92 ± 0.05***	0.83 ± 0.07	0.94 ± 0.03*	0.90 ± 0.05
	WM	0.78 ± 0.04***	0.68 ± 0.03	0.80 ± 0.03*	0.76 ± 0.06
	PCC	0.90 ± 0.06***	0.79 ± 0.05	0.98 ± 0.05	0.94 ± 0.05
Functional connectivity	SI-thal	0.38 ± 0.22***	0.01 ± 0.2	0.39 ± 0.24**	0.18 ± 0.25

*P < 0.05

**P < 0.01

***P < 0.001